Variance-Constrained Filter Design with Sensor Resolution under Round-Robin Communication Protocol: An Outlier-Resistant Mechanism

Hang Geng, Zidong Wang, Jun Hu, Qing-Long Han, and Yuhua Cheng

***Abstract*—In this paper, a new outlier-resistant mechanism is proposed to deal with the variance-constrained filtering problem for a class of networked systems subject to sensor resolution under the Round-Robin protocol (RRP). Sensor resolution, which serves as an important index in determining measurement accuracy, is taken into account in the addressed filtering problem, and the sensor-resolution-induced uncertainty is tackled by using an upper bounding technique. The RRP is employed to regulate the order of signal transmission in order to relieve communication overhead. In case of measurement outliers, a tailored saturation function is dedicatedly introduced to the filter structure for the purpose of suppressing the outlier-corrupted innovations, thereby maintaining satisfactory filtering performance. By solving a matrix difference equation, an upper bound is first acquired on the error covariance of the devised filter, and the associated filter parameters are subsequently determined through minimizing the acquired bound. The validity of the developed variance-constrained filter design approach is thoroughly demonstrated via two simulation examples.**

***Index Terms*—Variance-constrained filter, recursive filtering, sensor resolution, measurement outlier, Round-Robin protocol.**

I. Introduction

A central topic in signal processing is the filtering issue that has gained persistent research enthusiasm during the last few decades [5]–[7], [9], [11], [12], [16]. Filtering aims to reconstruct the signal of interest by making full use of available observations that might be contaminated by noises. Up till now, according to a wide variety of performance specifications, many filtering algorithms have been presented in the literature, among which the so-called recursive filtering approach has drawn particular research interest for its easy-to-implement nature [38]–[40]. Some typical recursive filtering approaches embrace the famous Kalman filter (KF) [8], extended KF [15], unscented KF [30], cubature KF [2], and Tobit KF [18], [31] algorithms, where the filtering error covariance is minimized at every iteration via properly designing associated filter parameters. For example, a variance-constrained recursive filtering algorithm has been devised in [45] for 2-D systems involving dynamical biases, random uncertainties and uniform quantization, where upper bounds on error covariances have been obtained and then minimized in the sense of matrix-trace.

It is well known that sensors are incapable of sensing arbitrarily small variation of the monitored object, and the smallest variation that a sensor can detect is referred to as sensor resolution [19], which is deemed as one of the most significant specifications on the accuracy of the sampled data. To be specific, a low (high) sensor resolution means that there is a large (small) deviation between the obtained sensor measurement and the real system measurement. The low sensor resolution, if inadequately handled, would undoubtedly give rise to biased sensor measurements leading to poor tracking performance. To solve sensor-resolution-induced (SRI) problems, some initial effort has been made in the area of target tracking where the main focus has been put on the establishment of an appropriate resolution model that can be integrated with the standard Bayesian tracking filter, see e.g. [41], [52]. Although the filtering problem under SRI effects has drawn some preliminary attention, the corresponding results have been very few when the filtering error covariance is of a major concern, and this constitutes one of the motivations for us to look into the variance-constrained filter design problem with sensor resolution.

For large-scale networked systems, sensor observations are sometimes subject to abnormal disturbances which are referred to as measurement outliers. Such outliers appear frequently in practice because of sensor aging (failures, faults or outages), sudden (unnoticed or unpredictable) external changes, and cyber-attacks launched by adversaries [4], [13], [33], [34], [46], [55]. Clearly, conventional filtering techniques are no longer effective here since the direct utilization of measurement outliers would lead to anomalies in innovations and subsequently out-of-range state estimates. As such, the so-called *outlier-resistant* recursive filters have recently attracted

This work was supported in part by the National Natural Science Foundation of China under Grant 62173068, Grant U21A2019, Grant 12171124, Grant 61933007, Grant 61973102, Grant U2030205, and Grant 61903065; in part by the Natural Science Foundation of Heilongjiang Province of China under Grant ZD2022F003; in part by the Natural Science Foundation of Sichuan Province of China under Grant 23NSFSC3603; in part by the Royal Society of the U.K.; and in part by the Alexander von Humboldt Foundation of Germany.
(Corresponding author: Zidong Wang.)

Hang Geng and Yuhua Cheng are with the School of Automation Engineering, University of Electronic Science and Technology of China, Chengdu 611731, China (emails: ghgoahead@126.com; yhcheng@uestc.edu.cn).

Zidong Wang is with the College of Electrical Engineering and Automation, Shandong University of Science and Technology, Qingdao 266590, China, and is also with the Department of Computer Science, Brunel University London, Uxbridge, Middlesex, UB8 3PH, United Kingdom (email: Zidong.Wang@brunel.ac.uk).

Jun Hu is with the Department of Mathematics, Harbin University of Science and Technology, Harbin 150080, China. He is also with the Key Laboratory of Advanced Manufacturing and Intelligent Technology, Ministry of Education, Harbin University of Science and Technology, Harbin 150080, China (email: jhu@hrbust.edu.cn).

Qing-Long Han is with the School of Science, Computing and Engineering Technologies, Swinburne University of Technology, Melbourne, VIC 3122, Australia (email: qhan@swin.edu.au).

a growing research interest with hope to guarantee the filter performance that is insensitive to the occurred outliers [1], [23]. For instance, a new observer has been built in [1] where a carefully designed strategy (for saturated output injection) has been adopted to attenuate the influence from measurement outliers on estimation performance. Nevertheless, the available outlier-related results on variance-constrained filters for networked systems have been very few, and this constitutes another motivation for the current investigation.

Nowadays, with the quick revolution of communication technologies, networked systems have been gaining increasing popularity because of the convenient cooperation/communication of the system components (e.g. sensors and filters) through shared networks [26], [28], [32], [37], [44], [49], [54]. Notice that the network bandwidth of a communication channel is inevitably limited, and this may cause various network-induced phenomena (NIP) such as data collision, network congestion, and packet dropout etc. [24], [27], [29], [35], [53]. As opposed to developing strategies that handle the occurred NIP [3], [36], [42], [48], a more *proactive* way in practice is to introduce adequate *communication protocols* to orchestrate the transmission order of the sensor data, thereby better utilizing the limited communication resource and preventing the NIP from taking place [10], [14], [17], [22], [47], [50], [51]. This situation gives rise to the third motivation of the present research.

In this paper, we endeavor to develop a new variance-constrained filter for a general class of networked systems undergoing complexities stemming jointly from sensor resolution, RRP scheduling and measurement outliers. Due to the existence of the underlying complexities, it is virtually difficult to assure the convergence of the resultant error covariance. As a result, we turn to seek for certain upper bounds on those error covariances (subject to variance constraints) with hope to ensure that the designed algorithm is non-divergent, and this constitutes another challenge of this paper. In addition, as the measurement contains the information of both sensor uncertainties and RRP scheduling, such information needs to be fully reflected in not only parameter determination but also performance investigation, and this constitutes the final challenge of this paper.

The primary contributions we are delivering can be outlined in threefold. *i) To our knowledge, we make one of the first few attempts here at designing a variance-constrained yet outlier-resistant filter under SRI effects and RRP scheduling, where both the system and the sensor models are holistically comprehensive in reflecting engineering practice. ii) In contrast to the existing recursive filters, an outlier-resistant mechanism is subtly embedded into the structure of the variance-constrained filter to curb adverse influences from outliers onto filtering accuracy. iii) A minimal upper bound is found to exist by rigorously parameterizing the filter to cope with the tight couplings between the SRI uncertainty, scheduling protocol as well as outlier-corrupted measurements.*

The rest of this paper is structured as follows. In Section II, we formulate the addressed variance-constrained filter design problem under the RRP, the measurement outlier and the sensor resolution. In Section III, a variance-constrained yet outlier-resistant filter is carefully designed with its parameters propitiously determined. In Section IV, examples about flight control and robot localization are given in order to showcase the usefulness of the proposed fusion framework, and a few conclusions are lastly drawn in Section V.

II. Problem Formulation

Consider the following discrete-time system:

$$x_{k+1} = A_k x_k + \omega_k, \tag{1}$$
$$z_k = C_k x_k + \upsilon_k \tag{2}$$

where $x_k \in \mathbb{R}^n$ is the state vector, $z_k \in \mathbb{R}^p$ is the measurement vector without considering sensor resolution, A_k and C_k are known matrices with compatible dimensions, and ω_k and υ_k are zero-mean, white, Gaussian noises in the process and the measurement with covariances Q_k and R_k, respectively. x_0 is the initial state of mean $\bar{x}_0$ and covariance P_{x_0}.

Definition 1: [52] Let $z_{i,k} \in \mathbb{R}$ $(i = 1, 2, \dots, p)$ be the ith element of z_k. If $z_{i,k}$ takes its value in the set $\{jr_i | j = 0, \pm 1, \dots, \pm m\}$ with $m > 0$ being a given integer, then

$$r \triangleq \begin{bmatrix} r_1 & r_2 & \cdots & r_p \end{bmatrix}^T \tag{3}$$

is the so-called sensor resolution where $r_i \in \mathbb{R}^+$ is the ith element of resolution r.

Assumption 1: The random variables υ_k, ω_k and x_0 are mutually uncorrelated.

In practical engineering, sensor i $(i = 1, 2, \dots, p)$ can only sense the measurement range that is larger than certain value, and this value (known as the sensor resolution) is given in Definition 1. Taking into consideration (3), the *actual* output of sensor i is

$$\bar{z}_{i,k} = \begin{cases} \left\lfloor \dfrac{z_{i,k}}{r_i} \right\rfloor r_i, & z_{i,k} \geq r_i, \\ 0, & z_{i,k} \in (-r_i, r_i), \\ \left\lceil \dfrac{z_{i,k}}{r_i} \right\rceil r_i, & z_{i,k} \leq -r_i \end{cases} \tag{4}$$

where $\lfloor \cdot \rfloor$ and $\lceil \cdot \rceil$ are the floor and ceiling functions, respectively. For sensor i, let us define the difference between its *actual* output $\bar{z}_{i,k}$ and ideal output $z_{i,k}$ by $\tilde{z}_{i,k} \triangleq \bar{z}_{i,k} - z_{i,k}$.

In the current investigation, sensor outputs $\bar{z}_{i,k} \in \mathbb{R}$ $(i = 1, 2, \dots, p)$ are transmitted to a remote estimator via a shared transmission network. To prevent data collision and improve the utilization efficiency of the communication resource, the RRP is used to schedule data communication in the sensor-to-estimator channel where all $\bar{z}_{i,k}$ are appointed equitable privileges to propagate through the communication network one-by-one in a circular way.

At time k, define the coefficient with respect to the measurement update by $\Gamma_{i,\hbar_k} \triangleq \delta(\hbar_k - i)$, and the selected sensor with transmission permission by $\hbar_k \triangleq \text{mod}(k-1, p) + 1 \in \{1, 2, \dots, p\}$ where $\text{mod}(k-1, p)$ stands for the non-negative remainder of $k - 1$ divided by p. Then, based on the zero-input strategy, at time k, the *final* measurement that reaches the filter is [16]

$$y_k = \sum_{i=1}^{p} \Gamma_{i,\hbar_k} \bar{z}_{i,k}. \tag{5}$$

In the previous section, it has been discussed that the outlier phenomenon of sensor measurements are widely encountered in practice which, if not adequately handled, would provoke abnormal measurement innovations and even render filter divergence. To mitigate detrimental effects from the outlier phenomenon, we deliberately introduce a saturation function $\sigma(\cdot)$ into the following filter structure:

$$\hat{x}_{k+1} = A_k\hat{x}_k + K_k\sigma(y_k - \hat{y}_k) \tag{6}$$

where $\hat{x}_k$ and $\hat{y}_k$ are the estimates of x_k and y_k, respectively, and $\hat{y}_k = \sum_{i=1}^{p}\Gamma_{i,\hbar_k}C_{i,k}\hat{x}_k$ where $C_{i,k}$ is the i-th entry of C_k. K_k is the filter gain to be designed. $\sigma(\cdot)$: $\mathbb{R}\mapsto\mathbb{R}$ is the saturation function defined by

$$\sigma(\tilde{y}_k) \triangleq \text{sign}(\tilde{y}_k)\text{min}\{|\tilde{y}_k|, \tilde{y}_k^{\max}\} \tag{7}$$

where $\tilde{y}_k \triangleq y_k - \hat{y}_k$ is the measurement innovation, and $\tilde{y}_k^{\max}$ is the known saturation level.

Now, let us present the derivation process of the measurement estimate $\hat{y}_k$. For sensor i, recalling $\tilde{z}_{i,k} \triangleq \bar{z}_{i,k} - z_{i,k}$, it is not difficult to obtain that $|\tilde{z}_{i,k}| < r_i$. Then, (5) becomes

$$y_k = \sum_{i=1}^{p}\Gamma_{i,\hbar_k}[\tilde{z}_{i,k} + (C_{i,k}x_k + \upsilon_{i,k})]$$

where $C_{i,k}$ and $\upsilon_{i,k}$ are the ith rows of C_k and υ_k, respectively. Noting the facts that $|\tilde{z}_{i,k}| < r_i$, $\hat{x}_k$ is defined as the estimate of x_k, and $\upsilon_{i,k}$ is a zero-mean Gaussian random variable, the estimates of $\tilde{z}_{i,k}$, x_k and $\upsilon_{i,k}$ can be determined as 0, $\hat{x}_k$ and 0, respectively. As such, the measurement estimate becomes

$$\hat{y}_k = \sum_{i=1}^{p}\Gamma_{i,\hbar_k}C_{i,k}\hat{x}_k.$$

Define the filtering error of filter (6) by $\tilde{x}_{k+1} \triangleq x_{k+1} - \hat{x}_{k+1}$. Consequently, we have the following error dynamics:

$$\tilde{x}_{k+1} = A_k\tilde{x}_k + \omega_k - K_k\sigma(y_k - \hat{y}_k). \tag{8}$$

Remark 1: In the sensor-to-estimator communication channel, measurements are possibly subject to outliers due to various kinds of reasons such as intermittent sensor failures, potential cyber-attacks and abrupt environment changes. In fact, measurement outliers are biased observations whose values significantly exceed the normal observation range, and this certainly provokes substantial deviations of the innovations from their normal values which, in turn, brings in adverse impacts on the final filtering performance. As such, in this paper, we are dedicated to designing an *outlier-resistant* filter (6) in order to achieve the desired filtering performance in the presence of the RRP and sensor resolution. It is observed from (7) that, via the introduction of a specific saturation function $\sigma(\cdot)$, the innovation is now constrained below a given saturation level $\tilde{y}_k^{\max}$ and, thus, the influence from outliers onto the filtering performance is mitigated. Basically, $\tilde{y}_k^{\max}$ can often be specified *a priori* in the light of our confidence/knowledge about possible sensor outputs in practical scenarios and, consequently, the filter (6) is said to be *outlier-resistant* where the function $\sigma(\cdot)$ is called *confidence-dependent*.

In this paper, we aim to devise an *outlier-resistant* filter (6) in the presence of the RRP and SRI effects such that 1) the error covariance $P_{\tilde{x}_k} \triangleq \mathbb{E}\{\tilde{x}_k\tilde{x}_k^T\}$ of filter (6) is ensured with an upper bound $\mathcal{P}_{\tilde{x}_k}$; and 2) the propitious gain of filter (6) is designed with minimized $\mathcal{P}_{\tilde{x}_k}$.

III. Main Results

This section is mainly dedicated to determining 1) an upper bound $\mathcal{P}_{\tilde{x}_{k+1}}$ in terms of solutions to a few matrix difference equations; and 2) a gain K_k that minimizes $\mathcal{P}_{\tilde{x}_k}$. The determination procedure exhibits the following two distinctive features: 1) a variance-constrained yet outlier-resistant filter scheme is presented which accommodates not only the measurement outliers but also the RRP effects; and (2) a few outlier-resistant terms (including the innovations, the covariance bounds as well as the filter gains) are all encompassed.

For sensor i, define the difference between measurements with and without sensor resolution by $\tilde{z}_{i,k} \triangleq \bar{z}_{i,k} - z_{i,k}$. To start with, two useful lemmas are presented as follows that would benefit the following derivations.

Lemma 1: [43] Define matrix functions by $\varrho_k(Y) : \mathbb{R}^{n\times n} \to \mathbb{R}^{n\times n}$ and $\rho_k(Y) : \mathbb{R}^{n\times n} \to \mathbb{R}^{n\times n}$ that satisfy

$$\varrho_k(Y) \leq \rho_k(Y) = \rho_k^T(Y), \varrho_k(Y) = \varrho_k^T(Y), \varrho_k(Y) \leq \varrho_k(X)$$

where $0 < Y = Y^T$ and $Y \leq X = X^T$. Then, under the initial condition $Y_0 = X_0 > 0$, there exist solutions Y_k and X_k to $Y_{k+1} = \varrho_k(Y_k), \quad X_{k+1} = \rho_k(X_k)$, such that $Y_k \leq X_k$ is true for $k \geq 0$.

Lemma 2: For sensor i, the difference $\tilde{z}_{i,k}$ satisfies the following condition:

$$|\tilde{z}_{i,k}| < r_i \tag{9}$$

where r_i is the known sensor resolution of sensor i.

Proof: The proof is straightforward and is thus omitted here. ∎

For any $\alpha, \beta \in \mathbb{R}^+$, define the following scalar function:

$$s(\alpha,\beta) = \begin{cases} 0, & \text{if } \alpha \leq \beta; \\ 1, & \text{otherwise.} \end{cases} \tag{10}$$

Taking advantage of (10), function (7) is rewritten as

$$\begin{aligned}\sigma(\tilde{y}_k) =& \tilde{y}_k\left[1 - s\left(|\tilde{y}_k|, \tilde{y}_k^{\max}\right)\right] \\ &+ \tilde{y}_k^{\max}\text{sign}(\tilde{y}_k)s\left(|\tilde{y}_k|, \tilde{y}_k^{\max}\right)\end{aligned} \tag{11}$$

which yields

$$\sigma(\tilde{y}_k) = d_kl_k + \tilde{y}_k(1 - d_k) \tag{12}$$

where

$$l_k \triangleq \tilde{y}_k^{\max}\text{sign}\left(\tilde{y}_k\right), d_k \triangleq s\left(\tilde{y}_k^{\max}, |\tilde{y}_k|\right).$$

Next, we calculate the error covariance $P_{\tilde{x}_{k+1}}$. Define the i-th $(i = 1, 2, \ldots, p)$ entry of R_k by $R_{i,k}$.

Theorem 1: The error covariance $P_{\tilde{x}_{k+1}}$ of filter (6) is

$$\begin{aligned}&P_{\tilde{x}_{k+1}} \\ =& \left[A_k - K_k\sum_{i=1}^{p}\Gamma_{i,\hbar_k}C_{i,k}\right]P_{\tilde{x}_k}\left[A_k - K_k\sum_{i=1}^{p}\Gamma_{i,\hbar_k}C_{i,k}\right]^T\end{aligned}$$

$$+\mathbb{E}\left\{d_kK_k\sum_{i=1}^{p}\Gamma_{i,\hbar_k}C_{i,k}\tilde{x}_k\left[d_kK_k\sum_{i=1}^{p}\Gamma_{i,\hbar_k}C_{i,k}\tilde{x}_k\right]^T\right\}$$
$$+\mathbb{E}\left\{K_kd_kl_k(K_kd_kl_k)^T\right\}+\mathbb{E}\left\{(1-d_k)K_k\sum_{i=1}^{p}\Gamma_{i,\hbar_k}\upsilon_{i,k}\right.$$
$$\left.\times\left[(1-d_k)K_k\sum_{i=1}^{p}\Gamma_{i,\hbar_k}\upsilon_{i,k}\right]^T\right\}+\mathbb{E}\left\{(1-d_k)K_k\right.$$
$$\left.\times\sum_{i=1}^{p}\Gamma_{i,\hbar_k}\tilde{z}_{i,k}\left[(1-d_k)K_k\sum_{i=1}^{p}\Gamma_{i,\hbar_k}\tilde{z}_{i,k}\right]^T\right\}$$
$$+\Pi_{1,k}+\Pi_{1,k}^T-\Pi_{2,k}-\Pi_{2,k}^T+\Pi_{3,k}+\Pi_{3,k}^T$$
$$-\Pi_{4,k}-\Pi_{4,k}^T-\Pi_{5,k}-\Pi_{5,k}^T+\Pi_{6,k}+\Pi_{6,k}^T$$
$$+\Pi_{7,k}+\Pi_{7,k}^T-\Pi_{8,k}-\Pi_{8,k}^T+Q_k \tag{13}$$

where

$$\Pi_{1,k}=\mathbb{E}\left\{\left[A_k-K_k\sum_{i=1}^{p}\Gamma_{i,\hbar_k}C_{i,k}\right]\tilde{x}_k\times\left[d_kK_k\sum_{i=1}^{p}\Gamma_{i,\hbar_k}C_{i,k}\tilde{x}_k\right]^T\right\}, \tag{14}$$

$$\Pi_{2,k}=\mathbb{E}\left\{\left[A_k-K_k\sum_{i=1}^{p}\Gamma_{i,\hbar_k}C_{i,k}\right]\tilde{x}_k\times\left[(1-d_k)K_k\sum_{i=1}^{p}\Gamma_{i,\hbar_k}\tilde{z}_{i,k}\right]^T\right\}, \tag{15}$$

$$\Pi_{3,k}=\mathbb{E}\left\{(1-d_k)K_k\sum_{i=1}^{p}\Gamma_{i,\hbar_k}\tilde{z}_{i,k}\times\left[(1-d_k)K_k\sum_{i=1}^{p}\Gamma_{i,\hbar_k}\upsilon_{i,k}\right]^T\right\}, \tag{16}$$

$$\Pi_{4,k}=\mathbb{E}\left\{d_kK_k\sum_{i=1}^{p}\Gamma_{i,\hbar_k}C_{i,k}\tilde{x}_k\times\left[(1-d_k)K_k\sum_{i=1}^{p}\Gamma_{i,\hbar_k}\tilde{z}_{i,k}\right]^T\right\}, \tag{17}$$

$$\Pi_{5,k}=\mathbb{E}\left\{d_kK_k\sum_{i=1}^{p}\Gamma_{i,\hbar_k}C_{i,k}\tilde{x}_k(K_kd_kl_k)^T\right\}, \tag{18}$$

$$\Pi_{6,k}=\mathbb{E}\left\{(1-d_k)K_k\sum_{i=1}^{p}\Gamma_{i,\hbar_k}\tilde{z}_{i,k}(K_kd_kl_k)^T\right\}, \tag{19}$$

$$\Pi_{7,k}=\mathbb{E}\left\{(1-d_k)K_k\sum_{i=1}^{p}\Gamma_{i,\hbar_k}\upsilon_{i,k}^T(K_kd_kl_k)^T\right\}, \tag{20}$$

$$\Pi_{8,k}=\mathbb{E}\left\{\left[A_k-K_k\sum_{i=1}^{p}\Gamma_{i,\hbar_k}C_{i,k}\right]\tilde{x}_k(K_kd_kl_k)^T\right\}. \tag{21}$$

Here, cross-terms $\Pi_{t,k}$ $(t=1,2,\ldots,8)$ in (15)–(21) along with the gain matrix K_{k+1} are to be determined later.

Proof: Paying attention to (2), (4), (5) and $\tilde{z}_{i,k}\triangleq\bar{z}_{i,k}-z_{i,k}$, we have

$$\tilde{y}_k=y_k-\hat{y}_k$$
$$=\sum_{i=1}^{p}\Gamma_{i,\hbar_k}\tilde{z}_{i,k}+\sum_{i=1}^{p}\Gamma_{i,\hbar_k}C_{i,k}\tilde{x}_k+\sum_{i=1}^{p}\Gamma_{i,\hbar_k}\upsilon_{i,k}, \tag{22}$$

by which error dynamics (8) is reformulated as

$$\tilde{x}_{k+1}=A_k\tilde{x}_k-K_k\sigma(\tilde{y}_k)+\omega_k$$
$$=\left[A_k-K_k\sum_{i=1}^{p}\Gamma_{i,\hbar_k}C_{i,k}\right]\tilde{x}_k+d_kK_k\sum_{i=1}^{p}\Gamma_{i,\hbar_k}C_{i,k}\tilde{x}_k$$
$$-K_kd_kl_k-(1-d_k)K_k\sum_{i=1}^{p}\Gamma_{i,\hbar_k}\tilde{z}_{i,k}$$
$$-(1-d_k)K_k\sum_{i=1}^{p}\Gamma_{i,\hbar_k}\upsilon_{i,k}+\omega_k. \tag{23}$$

Combining (23) and Assumption 1 yields

$$P_{\tilde{x}_{k+1}}$$
$$\triangleq\mathbb{E}\left\{\tilde{x}_{k+1}\tilde{x}_{k+1}^T\right\}$$
$$=\left[A_k-K_k\sum_{i=1}^{p}\Gamma_{i,\hbar_k}C_{i,k}\right]P_{\tilde{x}_k}\left[A_k-K_k\sum_{i=1}^{p}\Gamma_{i,\hbar_k}C_{i,k}\right]^T$$
$$+\mathbb{E}\left\{d_kK_k\sum_{i=1}^{p}\Gamma_{i,\hbar_k}C_{i,k}\tilde{x}_k\left[d_kK_k\sum_{i=1}^{p}\Gamma_{i,\hbar_k}C_{i,k}\tilde{x}_k\right]^T\right\}$$
$$+\mathbb{E}\left\{K_kd_kl_k(K_kd_kl_k)^T\right\}+\mathbb{E}\left\{(1-d_k)K_k\sum_{i=1}^{p}\Gamma_{i,\hbar_k}\upsilon_{i,k}\right.$$
$$\left.\times\left[(1-d_k)K_k\sum_{i=1}^{p}\Gamma_{i,\hbar_k}\upsilon_{i,k}\right]^T\right\}+\mathbb{E}\left\{(1-d_k)K_k\right.$$
$$\left.\times\sum_{i=1}^{p}\Gamma_{i,\hbar_k}\tilde{z}_{i,k}\left[(1-d_k)K_k\sum_{i=1}^{p}\Gamma_{i,\hbar_k}\tilde{z}_{i,k}\right]^T\right\}$$
$$+\Pi_{1,k}+\Pi_{1,k}^T-\Pi_{2,k}-\Pi_{2,k}^T+\Pi_{3,k}+\Pi_{3,k}^T$$
$$-\Pi_{4,k}-\Pi_{4,k}^T-\Pi_{5,k}-\Pi_{5,k}^T+\Pi_{6,k}+\Pi_{6,k}^T$$
$$+\Pi_{7,k}+\Pi_{7,k}^T-\Pi_{8,k}-\Pi_{8,k}^T+Q_k,$$

which is (13) where the cross-terms $\Pi_{t,k}$ $(t=1,2,\ldots,8)$ are given by (15)–(21). The proof is now complete. ■

Remark 2: Given the outlier-induced saturation innovation $\sigma(\tilde{y}_k)$, it is literally impossible to directly acquire the error covariance $P_{\tilde{x}_k}$ from error dynamics (8), but $P_{\tilde{x}_k}$ acts as an indispensable factor in determining our filter gain. In this regard, the saturation innovation $\sigma(\tilde{y}_k)$ is transformed into a linear combination of the innovation $\tilde{y}_k$ and the saturation level $\tilde{y}_k^{\max}$ so as to facilitate the derivation of the error covariance and filter gain. Thanks to such an innovation transformation, error dynamics (8) can be equally converted into a special structure that not only explicitly accommodates the RRP and SRI effects, but also greatly benefits the derivation of the expected $P_{\tilde{x}_{k+1}}$. Notice that, attributable to the emergence of a suite of complex cross-terms (e.g. $\Pi_{t,k}, t=1,2,\ldots,8$) in (13), it is technically difficult to find an explicit expression of the error covariance $P_{\tilde{x}_{k+1}}$. As such, in terms of matrix difference equations, we turn to explore the upper bound on such newly appeared cross-terms, and this leads to the desired upper bound as shown in the following theorem.

For known constant π_t $(t = 1, 2, \ldots, 8)$, we denote

$$a_1 = 1 + \pi_3^{-1} + \pi_7^{-1}, \tag{24}$$
$$a_2 = 1 + \pi_1 + \pi_2 + \pi_8^{-1}, \tag{25}$$
$$a_3 = 1 + \pi_1^{-1} + \pi_4^{-1} + \pi_5^{-1}, \tag{26}$$
$$a_4 = 1 + \pi_5 + \pi_6 + \pi_7 + \pi_8, \tag{27}$$
$$a_5 = 1 + \pi_2^{-1} + \pi_3 + \pi_4 + \pi_6^{-1}. \tag{28}$$

In line with (13)–(21), an explicit expression of the expected upper bound $\mathcal{P}_{\tilde{x}_{k+1}}$ on the error covariance (23) is given in the following theorem.

Theorem 2: Let the constants π_t $(t = 1, 2, \ldots, 8)$ and initial conditions $\mathcal{P}_{\tilde{x}_0} = P_{\tilde{x}_0} > 0$ be given. Then, the difference equation

$$\begin{aligned}
\mathcal{P}_{\tilde{x}_{k+1}} \triangleq & a_1 K_k \sum_{i=1}^{p} \Gamma_{i,\hbar_k}^2 [\text{tr}\{R_{i,k}\} I] K_k^T \\
& + a_2 \left[A_k - K_k \sum_{i=1}^{p} \Gamma_{i,\hbar_k} C_{i,k} \right] \\
& \times \mathcal{P}_{\tilde{x}_k} \left[A_k - K_k \sum_{i=1}^{p} \Gamma_{i,\hbar_k} C_{i,k} \right]^T + Q_k \\
& + a_3 K_k \sum_{i,k=1}^{p} \Gamma_{i,\hbar_k} C_{i,k} [\text{tr}\{\mathcal{P}_{\tilde{x}_k}\} I] C_{j,k}^T \Gamma_{j,\hbar_k} K_k^T \\
& + a_4 \left(\tilde{y}_k^{\max}\right)^2 K_k K_k^T + a_5 p \sum_{i=1}^{p} \Gamma_{i,\hbar_k}^2 r_i^2 K_k K_k^T
\end{aligned} \tag{29}$$

admits a solution $\mathcal{P}_{\tilde{x}_k}$ such that $\mathcal{P}_{\tilde{x}_k} \geq P_{\tilde{x}_k}$ holds for $k \geq 0$, that is, the error covariance $P_{\tilde{x}_k}$ is upper bounded by $\mathcal{P}_{\tilde{x}_k}$.

Proof: By means of the trace property and the matrix operation, we have

$$\begin{aligned}
\mathbb{E}\left\{K_k d_k l_k (K_k d_k l_k)^T\right\} \leq & K_k \mathbb{E}\left\{d_k l_k (d_k l_k)^T\right\} K_k^T \\
\leq & \left(\tilde{y}_k^{\max}\right)^2 K_k K_k^T,
\end{aligned} \tag{30}$$

$$\begin{aligned}
& \mathbb{E}\left\{ d_k K_k \sum_{i=1}^{p} \Gamma_{i,\hbar_k} C_{i,k} \tilde{x}_k \left[d_k K_k \sum_{j=1}^{p} \Gamma_{j,\hbar_k} C_{j,k} \tilde{x}_k \right]^T \right\} \\
\leq & K_k \sum_{i=1}^{p} \sum_{j=1}^{p} \Gamma_{i,\hbar_k} C_{i,k} [\text{tr}\{P_{\tilde{x}_k}\} I] C_{j,k}^T \Gamma_{j,\hbar_k} K_k^T,
\end{aligned} \tag{31}$$

$$\begin{aligned}
& \mathbb{E}\left\{ \mathbb{E}\left\{ (1-d_k)^2 K_k \sum_{i=1}^{p} \Gamma_{i,\hbar_k} \upsilon_{i,k} \left[K_k \sum_{i=1}^{p} \Gamma_{i,\hbar_k} \upsilon_{i,k} \right]^T \right\}\right\} \\
\leq & \sum_{i=1}^{p} \Gamma_{i,\hbar_k}^2 R_{i,k} K_k K_k^T,
\end{aligned} \tag{32}$$

$$\begin{aligned}
& \mathbb{E}\left\{ (1-d_k)^2 K_k \sum_{i=1}^{p} \Gamma_{i,\hbar_k} \tilde{z}_{i,k} \left[K_k \sum_{i=1}^{p} \Gamma_{i,\hbar_k} \tilde{z}_{i,k} \right]^T \right\} \\
\leq & K_k \sum_{i=1}^{p} \Gamma_{i,\hbar_k} \mathbb{E}\left\{\tilde{z}_{i,k} \tilde{z}_{i,k}^T\right\} \left[K_k \sum_{i=1}^{p} \Gamma_{i,\hbar_k} \right]^T \\
\leq & p \sum_{i=1}^{p} \Gamma_{i,\hbar_k}^2 r_i^2 K_k K_k^T
\end{aligned} \tag{33}$$

where the last inequality holds from Lemma 2.

For any constants π_t $(t = 1, 2, \ldots, 8)$, the cross-terms $\Pi_{t,k}$ in (15)–(18) satisfy

$$\begin{aligned}
\Pi_{1,k} + \Pi_{1,k}^T \leq & \pi_1 \left[A_k - K_k \sum_{i=1}^{p} \Gamma_{i,\hbar_k} C_{i,k} \right] P_{\tilde{x}_k} \\
& \times \left[A_k - K_k \sum_{k=1}^{p} \Gamma_{k,\hbar_k} C_{i,k} \right]^T + \pi_1^{-1} K_k \\
& \times \sum_{i=1}^{p} \sum_{j=1}^{p} \Gamma_{i,\hbar_k} C_{i,k} [\text{tr}\{P_{\tilde{x}_k}\} I] C_{j,k}^T \Gamma_{j,\hbar_k} K_k^T,
\end{aligned} \tag{34}$$

$$\begin{aligned}
\Pi_{2,k} + \Pi_{2,k}^T \leq & \pi_2 \left[A_k - K_k \sum_{i=1}^{p} \Gamma_{i,\hbar_k} C_{i,k} \right] P_{\tilde{x}_k} \\
& \times \left[A_k - K_k \sum_{i=1}^{p} \Gamma_{j,\hbar_k} C_{j,k} \right]^T \\
& + \pi_2^{-1} p r_i^2 \sum_{i=1}^{p} \Gamma_{i,\hbar_k}^2 K_k K_k^T,
\end{aligned} \tag{35}$$

$$\begin{aligned}
\Pi_{3,k} + \Pi_{3,k}^T \leq & \pi_3 p \sum_{i=1}^{p} \Gamma_{i,\hbar_k}^2 r_i^2 K_k K_k^T \\
& + \pi_3^{-1} K_k \sum_{i=1}^{p} \Gamma_{i,\hbar_k}^2 [\text{tr}\{R_{i,k}\} I] K_k^T,
\end{aligned} \tag{36}$$

$$\begin{aligned}
\Pi_{4,k} + \Pi_{4,k}^T \leq & \pi_4 p \sum_{i=1}^{p} \Gamma_{i,\hbar_k}^2 r_i^2 K_k K_k^T + \pi_4^{-1} K_k \sum_{i=1}^{p} \sum_{j=1}^{p} \\
& \times \Gamma_{i,\hbar_k} C_{i,k} [\text{tr}\{P_{\tilde{x}_k}\} I] C_{j,k}^T \Gamma_{j,\hbar_k} K_k^T,
\end{aligned} \tag{37}$$

$$\begin{aligned}
\Pi_{5,k} + \Pi_{5,k}^T \leq & \pi_5 \left(\tilde{y}_k^{\max}\right)^2 K_k K_k^T + \pi_5^{-1} K_k \sum_{i=1}^{p} \sum_{j=1}^{p} \\
& \times \Gamma_{i,\hbar_k} C_{i,k} [\text{tr}\{P_{\tilde{x}_k}\} I] C_{j,k}^T \Gamma_{j,\hbar_k} K_k^T,
\end{aligned} \tag{38}$$

$$\begin{aligned}
\Pi_{6,k} + \Pi_{6,k}^T \leq & \pi_6 \left(\tilde{y}_k^{\max}\right)^2 K_k K_k^T \\
& + \pi_6^{-1} p \sum_{i=1}^{p} \Gamma_{i,\hbar_k}^2 r_i^2 K_k K_k^T,
\end{aligned} \tag{39}$$

$$\begin{aligned}
\Pi_{7,k} + \Pi_{7,k}^T \leq & \pi_7 \left(\tilde{y}_k^{\max}\right)^2 K_k K_k^T \\
& + \pi_7^{-1} K_k \sum_{i=1}^{p} \Gamma_{i,\hbar_k}^2 [\text{tr}\{R_{i,k}\} I] K_k^T,
\end{aligned} \tag{40}$$

$$\begin{aligned}
\Pi_{8,k} + \Pi_{8,k}^T \leq & \pi_8 \left(\tilde{y}_k^{\max}\right)^2 K_k K_k^T \\
& + \pi_8^{-1} \left[A_k - K_k \sum_{i=1}^{p} \Gamma_{i,\hbar_k} C_{i,k} \right] \\
& \times P_{\tilde{x}_k} \left[A_k - K_k \sum_{j=1}^{p} \Gamma_{j,\hbar_k} C_{j,k} \right]^T.
\end{aligned} \tag{41}$$

Inserting (30)–(41) into (29), we have

$$P_{\tilde{x}_{k+1}} \leq a_1 K_k \sum_{i=1}^{p} \Gamma_{i,\hbar_k}^2 [\text{tr}\{R_{i,k}\} I] K_k^T$$

$$
\begin{aligned}
&+a_2\left[A_k-K_k\sum_{i=1}^{p}\Gamma_{i,\hbar_k}C_{i,k}\right]\\
&\times P_{\tilde{x}_k}\left[A_k-K_k\sum_{i=1}^{p}\Gamma_{i,\hbar_k}C_{i,k}\right]^T+Q_k\\
&+a_3K_k\sum_{i,j=1}^{p}\Gamma_{i,\hbar_k}C_{i,k}[\mathrm{tr}\{P_{\tilde{x}_k}\}I]C_{j,k}^T\Gamma_{j,\hbar_k}K_k^T\\
&+a_4\left(\tilde{y}_k^{\max}\right)^2K_kK_k^T+a_5p\sum_{i=1}^{p}\Gamma_{i,\hbar_k}^2r_i^2K_kK_k^T
\end{aligned}\tag{42}
$$

where a_i $(i=1,2,\cdots,5)$ are denoted in (24)-(28).

Inspired by (41) and (42), let us define matrix functions $\rho_k(P_{\tilde{x}_k}):\mathbb{R}^{n\times n}\to\mathbb{R}^{n\times n}$ and $\varrho_k(\mathcal{P}_{\tilde{x}_k}):\mathbb{R}^{n\times n}\to\mathbb{R}^{n\times n}$ by

$$
\begin{aligned}
&\mathcal{P}_{\tilde{x}_{k+1}}\\
\triangleq&\rho_k(\mathcal{P}_{\tilde{x}_k})\\
\triangleq&a_1K_k\sum_{i=1}^{p}\Gamma_{i,\hbar_k}^2[\mathrm{tr}\{R_{i,k}\}I]K_k^T\\
&+a_2\left[A_k-K_k\sum_{i=1}^{p}\Gamma_{i,\hbar_k}C_{i,k}\right]\\
&\times\mathcal{P}_{\tilde{x}_k}\left[A_k-K_k\sum_{i=1}^{p}\Gamma_{i,\hbar_k}C_{i,k}\right]^T+Q_k\\
&+a_3K_k\sum_{i,j=1}^{p}\Gamma_{i,\hbar_k}C_{i,k}[\mathrm{tr}\{\mathcal{P}_{\tilde{x}_k}\}I]C_{j,k}^T\Gamma_{j,\hbar_k}K_k^T\\
&+a_4\left(\tilde{y}_k^{\max}\right)^2K_kK_k^T+a_5p\sum_{i=1}^{p}\Gamma_{i,\hbar_k}^2r_i^2K_kK_k^T,
\end{aligned}\tag{43}
$$

$$
\begin{aligned}
&P_{\tilde{x}_{k+1}}\\
\triangleq&\varrho_k(P_{\tilde{x}_k})\\
\triangleq&\left[A_k-K_k\sum_{i=1}^{p}\Gamma_{i,\hbar_k}C_{i,k}\right]P_{\tilde{x}_k}\left[A_k-K_k\sum_{i=1}^{p}\Gamma_{i,\hbar_k}C_{i,k}\right]^T\\
&+\mathbb{E}\left\{d_kK_k\sum_{i=1}^{p}\Gamma_{i,\hbar_k}C_{i,k}\tilde{x}_k\left[d_kK_k\sum_{i=1}^{p}\Gamma_{i,\hbar_k}C_{i,k}\tilde{x}_k\right]^T\right\}\\
&+\mathbb{E}\left\{K_kd_kl_k(K_kd_kl_k)^T\right\}+\mathbb{E}\left\{(1-d_k)K_k\sum_{i=1}^{p}\Gamma_{i,\hbar_k}\upsilon_{i,k}\right.\\
&\left.\times\left[(1-d_k)K_k\sum_{i=1}^{p}\Gamma_{i,\hbar_k}\upsilon_{i,k}\right]^T\right\}+\mathbb{E}\left\{(1-d_k)K_k\right.\\
&\left.\times\sum_{i=1}^{p}\Gamma_{i,\hbar_k}\tilde{z}_{i,k}\left[(1-d_k)K_k\sum_{i=1}^{p}\Gamma_{i,\hbar_k}\tilde{z}_{i,k}\right]^T\right\}\\
&+\Pi_{1,k}+\Pi_{1,k}^T-\Pi_{2,k}-\Pi_{2,k}^T+\Pi_{3,k}+\Pi_{3,k}^T\\
&-\Pi_{4,k}-\Pi_{4,k}^T-\Pi_{5,k}-\Pi_{5,k}^T+\Pi_{6,k}+\Pi_{6,k}^T\\
&+\Pi_{7,k}+\Pi_{7,k}^T-\Pi_{8,k}-\Pi_{8,k}^T+Q_k.
\end{aligned}\tag{44}
$$

Bearing (43)–(44) in mind, one verifies that $\varrho_k(P_{\tilde{x}_k})$ and $\rho_k(\mathcal{P}_{\tilde{x}_k})$ satisfy conditions in Lemma 1. Consequently, given $\mathcal{P}_{\tilde{x}_0}=P_{\tilde{x}_0}>0$, it is concluded that there exist solutions $\mathcal{P}_{\tilde{x}_k}$ and $P_{\tilde{x}_k}$ to $\mathcal{P}_{\tilde{x}_{k+1}}=\rho_k(\mathcal{P}_{\tilde{x}_k})$ and $P_{\tilde{x}_{k+1}}=\varrho_k(P_{\tilde{x}_k})$ such that $P_{\tilde{x}_k}\le\mathcal{P}_{\tilde{x}_k}$ is true for $k\ge 0$, i.e. $P_{\tilde{x}_k}$ is upper bounded by $\mathcal{P}_{\tilde{x}_k}$, which completes the proof. ■

It is found from Definition 1 and Lemma 2 that 1) the sensor resolution is a specification index that evaluates the error between the real and sampled sensor data, where a low (high) sensor resolution means that there is a large (small) error between the obtained sensor measurement and the real system measurement; and 2) for each sensor i, its sensor resolution induced error is restricted by an upper bound r_i. Since a large (small) measurement error often leads to a large (small) filtering error covariance, we conclude that a large (small) r_i results in a bad (good) filtering performance. Such a conclusion is later verified by Theorem 2 in our main results, from which one confirms that r_i is a paramount parameter in the determination of the bound that confines the resultant filtering error covariance, and a large (small) r_i implies a high (low) bound on the error covariance, giving rise to a bad (good) performance of the designed filter.

Remark 3: It will be shown in Theorem 3 that the upper bound $\mathcal{P}_{\tilde{x}_{k+1}}$ presented in Theorem 2 can be rewritten as (49) which further leads to the minimum upper bound $\mathcal{P}_{\tilde{x}_{k+1}}^{\min}$ by properly designing the filter gain K_k as (45). This certainly verifies that $\mathcal{P}_{\tilde{x}_{k+1}}$ is lower bounded by $\mathcal{P}_{\tilde{x}_{k+1}}^{\min}$. Note that in terms of boundedness, we are more interested in exploring the bondedness of $\mathcal{P}_{\tilde{x}_{k+1}}^{\min}$ due to the reason that it guarantees the proper filter gain as well as the expected locally optimal performance of the designed filter. Theorem 3 will illustrate that the structure of $\mathcal{P}_{\tilde{x}_{k+1}}^{\min}$ is similar to that of the filtering error covariance in Kalman-like filters (see references [25], [56]), and thus it is not difficult to find both upper and lower bounds on $\mathcal{P}_{\tilde{x}_{k+1}}^{\min}$ by taking advantage of the boundedness analysis procedure presented in [25], [56], where certain boundedness assumptions on saturation levels $\tilde{y}_k^{\max}$ and matrices Q_k, $R_{i,k}$, $A_kA_k^T$ and $C_{i,k}C_{i,k}^T$ should be made.

Next, we endeavor to minimize the bound attained in (29) so as to achieve the expected filter gain.

Theorem 3: Let the constants $a_{t,k}$ $(t=1,2,\ldots,5)$ be given. Then, the bound given by (29) is minimized via designing the gain K_k as

$$K_k=\Xi_k\Pi_k^{-1},\tag{45}$$

where

$$\Xi_k\triangleq a_2A_k\mathcal{P}_{\tilde{x}_k}\sum_{i=1}^{p}C_{i,k}^T\Gamma_{i,\hbar_k},\tag{46}$$

$$
\begin{aligned}
\Pi_k\triangleq\ &a_1\sum_{i=1}^{p}\Gamma_{i,\hbar_k}^2[\mathrm{tr}\{R_{i,k}\}I]\\
&+a_2\sum_{i=1}^{p}\sum_{j=1}^{p}\Gamma_{i,\hbar_k}C_{i,k}\mathcal{P}_{\tilde{x}_k}C_{j,k}^T\Gamma_{j,\hbar_k}\\
&+a_3\sum_{i=1}^{p}\sum_{j=1}^{p}\Gamma_{i,\hbar_k}C_{i,k}[\mathrm{tr}\{\mathcal{P}_{\tilde{x}_k}\}I]C_{j,k}^T\Gamma_{j,\hbar_k}\\
&+a_4\left(\tilde{y}_k^{\max}\right)^2I+a_5p\sum_{i=1}^{p}\Gamma_{i,\hbar_k}^2r_i^2I.
\end{aligned}\tag{47}
$$

Furthermore, the minimal bound $\mathcal{P}^{\min}_{\tilde{x}_{k+1}}$ is

$$\mathcal{P}^{\min}_{\tilde{x}_{k+1}} = a_2 A_k \mathcal{P}_{\tilde{x}_k} A_k^T + Q_k - \Xi_k \Pi_k^{-1} \Xi_k^T. \tag{48}$$

Proof: The bound $\mathcal{P}_{\tilde{x}_{k+1}}$ in (29) can be converted into the following structure:

$$\begin{aligned}\mathcal{P}_{\tilde{x}_{k+1}} =& a_2 A_k \mathcal{P}_{\tilde{x}_k} A_k^T + Q_k + K_k \Pi_k K_k^T \\ &- K_k \Xi_k^T - \Xi_k K_k^T \\ =& a_2 A_k \mathcal{P}_{\tilde{x}_k} A_k^T + Q_k - \Xi_k \Pi_k^{-1} \Xi_k^T \\ &+ (K_k - \Xi_k \Pi_k^{-1}) \Pi_k (K_k - \Xi_k \Pi_k^{-1})^T \end{aligned} \tag{49}$$

where Ξ_k and Π_k are defined by (46) and (47), respectively.

It follows from (49) that, if K_k takes the form of (45), i.e. $K_k = \Xi_k \Pi_k^{-1}$, then $\mathcal{P}_{\tilde{x}_{k+1}}$ achieves its minimal value as given by (46), and the proof is complete. ∎

Remark 4: In this paper, a variance-constrained filter design problem is concerned with sensor resolution under the RRP. A novel outlier-resistant mechanism is proposed to cope with the possible measurement outliers where an saturation structure is introduced to constrain the outlier effect onto the measurement innovation. Later on, the saturated innovation $\sigma(\tilde{y}_k)$ is transformed into a linear combination of the innovation $\tilde{y}_k$ and the saturation level $\tilde{y}_k^{\max}$ so as to facilitate subsequent filter parameterization. An upper bound on the SRI uncertainty (i.e. the difference between measurements with and without sensor resolution) is then successfully attained in Lemma 2. Subsequently, the error covariance of the filter is acquired and minimized in Theorems 1–2 with the propitious gain parameter found in Theorem 3. It is worth mentioning that the obtained minimal bound reflects all information from the underlying system undergoing sensor resolution, measurement outlier and RRP scheduling.

Remark 5: So far, the variance-constrained filtering algorithm has been well formulated for networked systems in the presence of multiple observation uncertainties that encompass outliers, stochastic noises and sensor resolution under the RRP. A careful observation of the primary results outlined in Lemma 2 and Theorems 1–3 tells that all involved uncertainties together with the RRP that contribute to our system complexity are explicitly reflected in our filter design and analysis procedures. In comparison with the existing literature, the main results of this paper owns the following distinctive characteristics: 1) the networked filtering problem discussed here is new in the sense that the sensor resolution, measurement outliers and RRP are taken into careful consideration; 2) a variance-constrained yet outlier-resistant filtering scheme is devised to resolve the mathematical complexities stemming from SRI uncertainties and outlier-corrupted measurements; and 3) the performance of our developed filtering algorithm is testified through two practical examples as shown in the following section.

IV. Illustrative Examples

In this section, we leverage two examples about flight control (modified from [21]) and robot localization (modified from [20]) to elucidate the applicability of the presented filter design strategy and performance analysis mechanism.

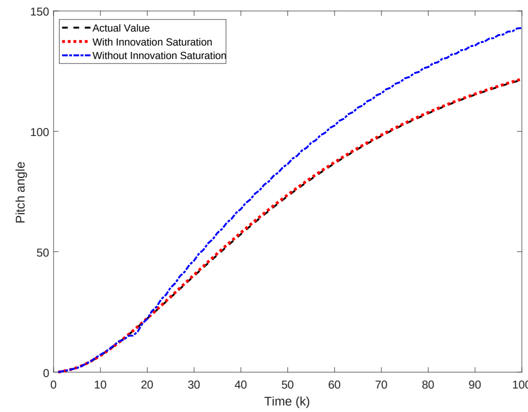

Fig. 1: True and estimated trajectories of pitch angle.

For the sth $(s = 1, 2, \ldots, n)$ entry of x_k (defined by x_k^s), its root mean-squared error (RMSEs) is defined by

$$\text{RMSE}s \triangleq \sqrt{\frac{1}{M} \sum_{j=1}^{M} \left(x_k^{s(j)} - \hat{x}_k^{s(j)} \right)^2}$$

where $M = 500$ is the number of Monte Carlo trials and $k = 100$ is the time step in each trial. The mean squared error of x_k is defined by

$$\text{MSE} \triangleq \frac{1}{M} \sum_{j=1}^{M} \left(\left(\tilde{x}_k^{(j)} \right)^T \tilde{x}_k^{(j)} \right).$$

For all conducted simulations, the sampling sensor is subject to sensor resolution, the measurement transmission is scheduled via the RRP, and the collected measurements are corrupted by possible outliers taking the form of a disturbance signal o_k. In the sequel, examples on both flight control and robot localization are leveraged to testify the robustness of our filter against outliers, where several performance comparisons are made between the proposed outlier-resistant filter with innovation saturation and the outlier-corrupted filter without innovation saturation.

A. Example of Flight Control

Consider a longitudinal flight control model:

$$\begin{aligned} x_{k+1} =& A_k x_k + B_k u_k + \omega_k, \\ z_k =& C_k x_k + v_k \end{aligned}$$

where x_k is the flight state consisting of the pitch angle $x_{1,k}$, pitch rate $x_{2,k}$ as well as normal velocity $x_{3,k}$, and u_k is the given input of elevator control.

$$A_k = \begin{bmatrix} 0.9944 & -0.1203 & -0.4302 \\ 0.0017 & 0.9902 & -0.0747 \\ 0 & 0.8187 & 0 \end{bmatrix}, \tilde{y}_k^{\max} = \begin{bmatrix} 30 \\ 5 \\ 5 \end{bmatrix},$$

$$B_k = \begin{bmatrix} 0.4252 \\ -0.0082 \\ 0.1813 \end{bmatrix}, o_k = \begin{cases} 10e, & 20 < k < 40, \\ 10e \sin(w) & 50 < k < 70, \\ 10e \cos(w), & 80 < k < 100, \end{cases}$$

$$Q_k = 0.01 I_3, R_k = 0.01 I_3, P_{x_0} = 0.01 I_3, \bar{x}_0 = \begin{bmatrix} 0 & 0 & 0 \end{bmatrix}^T,$$

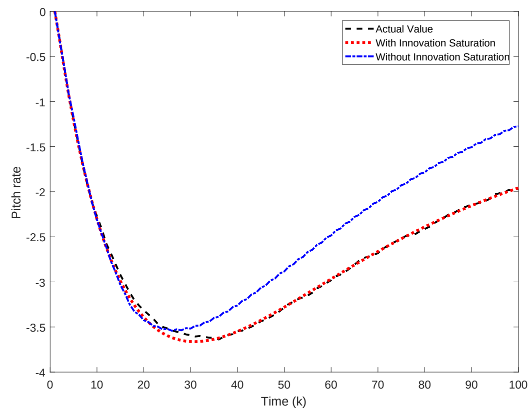

Fig. 2: True and estimated trajectories of pitch rate.

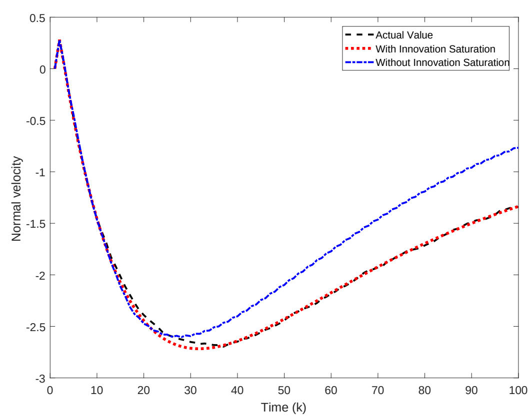

Fig. 3: True and estimated trajectories of normal velocity.

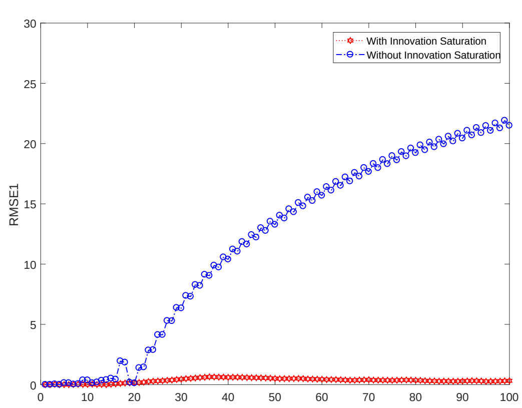

Fig. 4: RMSE of pitch angle.

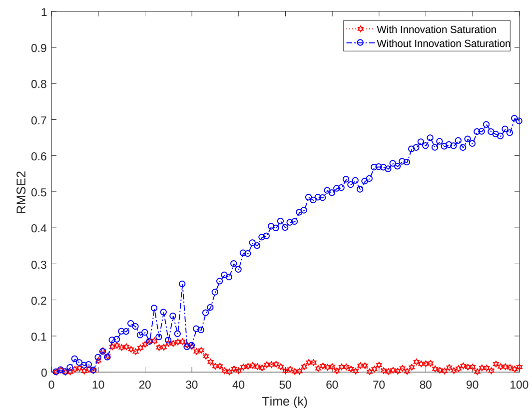

Fig. 5: RMSE of pitch rate.

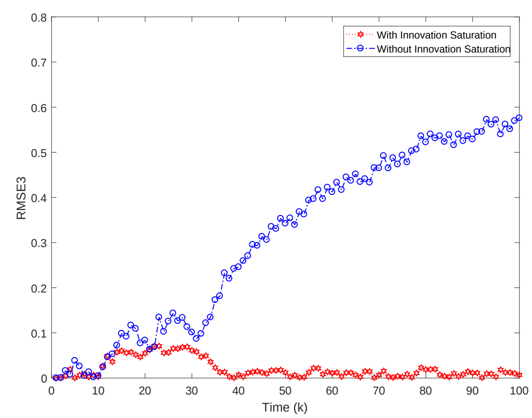

Fig. 6: RMSE of normal velocity.

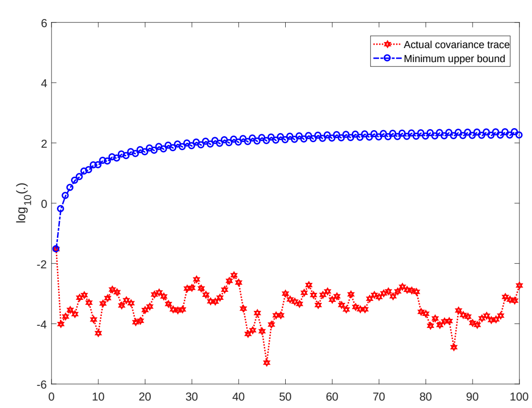

Fig. 7: Comparison: $\log_{10}\left(\mathrm{tr}\{P_{\tilde{x}_k}^{\min}\}\right)$ and $\log_{10}\left(\mathrm{tr}\{\mathcal{P}_{\tilde{x}_k}^{\min}\}\right)$.

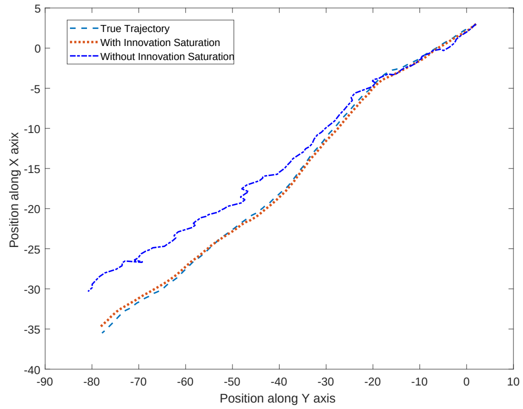

Fig. 8: Robot position: true and estimated trajectories.

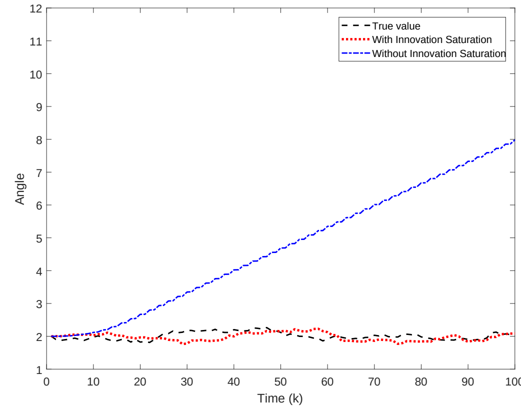

Fig. 9: Robot angle: true and estimated trajectories.

$$C_k = I_3, r_1 = 20, r_2 = 2, r_3 = 1, \pi_1 = 1.0, \pi_2 = 0.5, u_k = 10,$$
$$\pi_3 = 0.5, \pi_4 = 0.3, \pi_5 = 0.2, \pi_6 = 0.7, \pi_7 = 0.4, \pi_8 = 0.3$$

where $w = 0.052\pi$ and $e = \begin{bmatrix} 1 & 1 & 1 \end{bmatrix}^T$. Convert the flight control model into

$$x_{k+1} = A_k x_k + \tilde{\omega}_k,$$
$$z_k = C_k x_k + \upsilon_k,$$

where $\tilde{\omega}_k = B_k u_k + \omega_k$ can be equivalently treated as a Gaussian noise of mean $B_k u_k$ along with covariance Q_k.

Figs. 1–3 depict trajectories of the pitch angle $x_{1,k}$, pitch rate $x_{2,k}$, normal velocity $x_{3,k}$ and their estimates $\hat{x}_{1,k}$, $\hat{x}_{2,k}$ and $\hat{x}_{3,k}$, and Figs. 4–6 plot associated RMSEs. One observers explicitly from Figs. 1–3 that estimation curves produced by the filter with innovation saturation almost coincide with the true state curves, while estimation curves produced by the filter without innovation saturation have large deviations from true state curves. It is apparently seen from Figs. 4–6 that RMSE curves generated by the filter with innovation saturation always reside lower than that generated by the filter without innovation saturation.

Additionally, Fig. 7 sketches variation trends of trace curves with respect to $P_{\tilde{x}_k}$ and $\mathcal{P}^{\min}_{\tilde{x}_k}$ where the values of $P_{\tilde{x}_k}$ are approximated by the corresponding MSE values due to the impossibility of analytically computing the error covariance. One observes explicitly from Fig. 7 that values of $\log_{10}(\mathrm{tr}\{P_{\tilde{x}_k}\})$ are always smaller than that of $\log_{10}\left(\mathrm{tr}\{\mathcal{P}^{\min}_{\tilde{x}_k}\}\right)$. The above demonstration figures apparently elucidate the robustness of the filter with innovation saturation against outliers and the correctness of the upper bound result claimed in Lemma 2 and Theorems 1–3.

B. *Example of Robot Localization*

Consider a robot localization scenario taken place in a 2D $\vec{X}-\vec{Y}$ plane, and the kinetic model of the mobile robot is characterized by system (1). The state of the robot consists of the position $x_{1,k}$ along the $\vec{X}$ axis, the position $x_{2,k}$ along the $\vec{Y}$ axis and the angle $x_{3,k}$ between the $\vec{X}$ axis and the forward

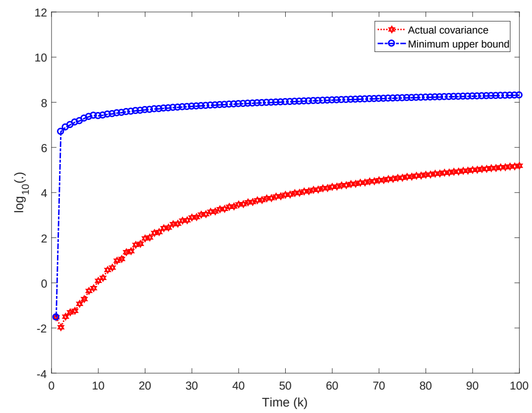

Fig. 10: Comparison: $\log_{10}\left(\mathrm{tr}\{P^{\min}_{\tilde{x}_k}\}\right)$ and $\log_{10}\left(\mathrm{tr}\{\mathcal{P}^{\min}_{\tilde{x}_k}\}\right)$.

axis of the robot. The process noise ω_k has a covariance $Q_k = \mathrm{diag}\{0.05, 0.05, 0.05\}$, and the state transition matrix is

$$A_k = \begin{bmatrix} 1 & 0 & -u_k \sin(\hat{x}_{3,k-1}) \\ 0 & 1 & u_k \cos(\hat{x}_{3,k-1}) \\ 0 & 0 & 1 \end{bmatrix}$$

where $u_k = \nu_k T$, $T = 150$ ms is the sampling interval and $\nu_k = 30$ mm/s is the displacement velocity of the robot.

In this example, two sensors with resolution $r_1 = 10$ and resolution $r_2 = 1$ are deployed to collect the robot information. The collected measurements before sensor resolution are described by system (2) where the measurement noise has a covariance $R_k = I_2$. The measurement transition matrix is

$$C_k = \begin{bmatrix} -\frac{l_1 - x_{1,k-1}}{f_k} & -\frac{l_2 - x_{2,k-1}}{f_k} & 0 \\ \frac{l_2 - x_{2,k-1}}{f_k^2} & -\frac{l_1 - x_{1,k-1}}{f_k^2} & 1 \end{bmatrix},$$
$$f_k = \sqrt{(l_1 - x_{1,k})^2 + (l_2 - x_{2,k})^2}$$

where (l_1, l_2) is the position of the landmark point. In the simulation, we set $x_{1,0} = 2$ m, $x_{2,0} = 3$ m, $x_{3,0} = 2$ rad/s, $P_{\tilde{x}_0} = 0.01 I_3$, $l_1 = 5$ m and $l_2 = 5$ m. The outlier signal is set as $0_k = 30h$ for $0 < k < 30$, $o_k = 30h\sin(wT)$ for

$30 < k < 60$ and $o_k = 30h\cos(wT)$ for $70 < k < 100$ where $h = \begin{bmatrix}1 & 1\end{bmatrix}^T$.

The simulation results are given in Figs. 8–10 where Figs. 8–9 show the actual and estimated trajectories of both robot position and angle, while Fig. 10 plots the trace curves of the error covariance $P_{\tilde{x}_{k+1}}$ and its minimal bound $\mathcal{P}^{\min}_{\tilde{x}_{k+1}}$. These simulation results apparently verify the correctness of the results presented in Lemma 2 and Theorems 1–3, and the applicability of such results in the scenario of robot localization.

V. Conclusion

In this paper, we have addressed the variance-constrained filtering problem for networked systems in the presence of the sensor resolution and RRP. A novel outlier-resistant structure has been devised in which a saturation function has been deployed to restrict the outlier influence on measurement innovations, thereby keeping the satisfactory performance of our variance-constrained filter. By solving matrix difference equations, upper bounds on the resultant error covariances have been acquired, and associated filter gains have been subsequently determined through minimizing such bounds. Finally, simulation examples on flight control and mobile robot have been exploited to validate the effectiveness of the designed filter. Some future research directions are 1) the variance-constrained filter design problem under other communication protocols, e.g. the random access protocol and the try-once-discard protocol; and 2) he variance-constrained filter design problem under other measurement disturbances, for example, sensor bias and sensor saturation.

References

[1] A. Alessandri, and L. Zaccarian, Stubborn state observers for linear time-invariant systems, *Automatica*, vol. 88, pp. 1–9, 2018.

[2] I. Arasaratnam, and S. Haykin, Cubature Kalman filters, *IEEE Transactions on Automatic Control*, vol. 54, no. 6, pp. 1254–1269, 2009.

[3] G. Bao, L. Ma and X. Yi, Recent advances on cooperative control of heterogeneous multi-agent systems subject to constraints: A survey, *Systems Science & Control Engineering*, vol. 10, no. 1, pp. 539-551, 2022.

[4] V. P. Bhuvana, C. Preissl, A. M. Tonello, and M. Huemer, Multi-sensor information filtering with information-based sensor selection and outlier rejection, *IEEE Sensors Journal*, vol. 18, no. 6, pp. 2442–2452, 2018.

[5] R. Caballero-Águila, A. Hermoso-Carazo, and J. Linares-Pérez, Networked fusion estimation with multiple uncertainties and time-correlated channel noise, *Information Fusion*, vol. 54, pp. 161–171, 2020.

[6] R. Caballero-Águila, A. Hermoso-Carazo, and J. Linares-Pérez, Networked distributed fusion estimation under uncertain outputs with random transmission delays, packet losses and multi-packet processing, *Signal Processing*, vol. 156, pp. 71–83, 2019.

[7] B. Chen, D. W. C. Ho, G. Hu, and L. Yu, Secure fusion estimation for bandwidth constrained cyber-physical systems under replay attacks, *IEEE Transactions on Cybernetics*, vol. 48, no. 6, pp. 1862–1876, 2018.

[8] B. Chen, G. Hu, D. W. C. Ho, and L. Yu, Distributed Kalman filtering for time-varying discrete sequential systems, *Automatica*, vol. 99, pp. 228–236, 2019.

[9] Y. Chen, K. Ma, and R. Dong, Dynamic anti-windup design for linear systems with time-varying state delay and input saturations, *International Journal of Systems Science*, vol. 53, no. 10, pp. 2165-2179, 2022.

[10] Y. Chen, Q. Song, Z. Zhao, Y. Liu, and F. E. Alsaadi, Global Mittag-Leffler stability for fractional-order quaternion-valued neural networks with piecewise constant arguments and impulses, *International Journal of Systems Science*, vol. 53, no. 8, pp. 1756-1768, 2022.

[11] D. Ciuonzo, A. Aubry, and V. Carotenuto, Rician MIMO channel- and jamming-aware decision fusion, *IEEE Transactions on Signal Processing*, vol. 65, no. 15, pp. 3866–3880, 2017.

[12] D. Ciuonzo, V. Carotenuto, and A. De Maio, On multiple covariance equality testing with application to SAR change detection, *IEEE Transactions on Signal Processing*, vol. 65, no. 19, pp. 5078–5091, 2017.

[13] J. Dai, and H. C. So, Sparse Bayesian learning approach for outlier-resistant direction-of-arrival estimation, *IEEE Transactions on Signal Processing*, vol. 66, no. 3, pp. 744–756, 2017.

[14] Y. Dong, Y. Song, and G. Wei, Efficient model-predictive control for networked interval type-2 T-S fuzzy system with stochastic communication protocol, *IEEE Transactions on Fuzzy Systems*, vol. 29, no. 2, pp. 286–297, 2021.

[15] P. Frogerais, J.-J. Bellanger, and L. Senhadji, Various ways to compute the continuous-discrete extended Kalman filter, *IEEE Transactions on Automatic Control*, vol. 57, no. 4, pp. 1000–1004, 2012.

[16] H. Geng, Z. Wang, X. Yi, F. E. Alsaadi, and Y. Cheng, Tobit Kalman filtering for fractional-order systems with stochastic nonlinearities under Round-Robin protocol, *International Journal of Robust and Nonlinear Control*, vol. 31, pp. 2348–2370, 2021.

[17] H. Geng, Z. Wang, F. E. Alsaadi, K. H. Alharbi, and Y. Cheng, Protocol-based fusion estimator design for state-saturated systems with dead-zone-like censoring under deception attacks, *IEEE Transactions on Signal and Information Processing over Networks*, vol. 8, pp. 37–48, 2022.

[18] H. Geng, Z. Wang, L. Zou, A. Mousavi, and Y. Cheng, Protocol-based Tobit Kalman filter under integral measurements and probabilistic sensor failures, *IEEE Transactions on Signal Processing*, vol. 69, pp. 546–559, 2021.

[19] G. Hemalakshmi, D. Santhi, V. Mani, A. Geetha, and N. Prakash, Deep residual network based on image priors for single image super resolution in FFA Images, *CMES-Computer Modeling in Engineering & Sciences*, vol. 125, no. 1, pp. 125–143, 2020.

[20] L. Jetto, S. Longhi, and G. Venturini, Development and experimental validation of an adaptive extended Kalman filter for the localization of mobile robots, *IEEE Transactions on Robotics and Automation*, vol. 15, no. 2, pp. 219–229, 1999.

[21] K. Khémiri, F. Hmida, J. Ragot, and M. Gossa, Novel optimal recursive filter for state and fault estimation of linear stochastic systems with unknown disturbances, *International Journal of Applied Mathematics and Computer Science*, vol. 21, no. 4, pp. 629–637, 2011.

[22] J. Li, G. Wei, D. Ding and E. Tian, Protocol-based H_∞ filtering for piecewise linear systems: A measurement-dependent equivalent reduction approach, *International Journal of Robust and Nonlinear Control*, vol. 31, no. 8, pp. 3163–3178, 2021.

[23] J. Li, Z. Wang, H. Dong, and G. Ghinea, Outlier-resistant remote state estimation for recurrent neural networks with mixed time-delays, *IEEE Transactions on Neural Networks and Learning Systems*, vol. 32, no. 5, pp. 2266-2273, 2021.

[24] W. Li, Y. Niu and Z. Cao, Event-triggered sliding mode control for multi-agent systems subject to channel fading, *International Journal of Systems Science*, vol. 53, no. 6, pp. 1233–1244, 2022.

[25] W. Li, Z. Wang, D. W. C. Ho, and G. Wei, On boundedness of error covariances for Kalman consensus filtering problems, *IEEE Transactions on Automatic Control*, vol. 65, no. 6, pp. 2654–2661, 2020.

[26] X. Li, Q. Song, Y. Liu, and F. E. Alsaadi, Nash equilibrium and bang-bang property for the non-zero-sum differential game of multi-player uncertain systems with Hurwicz criterion, *International Journal of Systems Science*, vol. 53, no. 10, pp. 2207-2218, 2022.

[27] X. Li, Q. Song, Z. Zhao, Y. Liu, and F. E. Alsaadi, Optimal control and zero-sum differential game for Hurwicz model considering singular systems with multifactor and uncertainty, *International Journal of Systems Science*, vol. 53, no. 7, pp. 1416–1435, 2022.

[28] K. Liu, H. Guo, Q. Zhang, and Y. Xia, Distributed secure filtering for discrete-time systems under Round-Robin protocol and deception attacks. *IEEE Transactions on Cybernetics*, vol. 50, no. 8, pp. 3571–3580, 2020.

[29] P. Wen, X. Li, N. Hou, and S. Mu, Distributed recursive fault estimation with binary encoding schemes over sensor networks, *Systems Science & Control Engineering*, vol. 10, no. 1, pp. 417–427, 2022.

[30] S. Liu, Z. Wang, Y. Chen and G. Wei, Protocol-based unscented Kalman filtering in the presence of stochastic uncertainties, *IEEE Transactions on Automatic Control*, vol. 65, no. 3, pp. 1303–1309, 2020.

[31] K. Loumponias, N. Vretos, G. Tsaklidis, and P. Daras, An improved Tobit Kalman filter with adaptive censoring limits, *Circuits, Systems, and Signal Processing*, vol. 39, pp. 5588–5617, 2020.

[32] O. Mahdi, F. Eshghi, and A. Zamani, A hybrid encryption algorithm for security enhancement of wireless sensor networks: A supervisory approach to pipelines, *CMES-Computer Modeling in Engineering & Sciences*, vol. 122, no. 1, pp. 323–349, 2020.

[33] H.-Q. Mu, and K.-V. Yuen, Novel outlier-resistant extended Kalman filter for robust online structural identification, *Journal of Engineering Mechanics*, vol. 141, no. 1, art. no. 04014100, 2015.

[34] H. Park, Outlier-resistant high-dimensional regression modelling based on distribution-free outlier detection and tuning parameter selection, *Journal of Statistical Computation and Simulation*, vol. 87, no. 9, pp. 1799–1812, 2017.

[35] B. Qu, B. Shen, Y. Shen, and Q. Li, Dynamic state estimation for islanded microgrids with multiple fading measurements, *Neurocomputing*, vol. 406, pp. 196–203, 2020.

[36] F. Qu, X. Zhao, X. Wang and E. Tian, Probabilistic-constrained distributed fusion filtering for a class of time-varying systems over sensor networks: a torus-event-triggering mechanism, *International Journal of Systems Science*, vol. 53, no. 6, pp. 1288–1297, 2022.

[37] S. Roshany-Yamchi, M. Cychowski, R. R. Negenborn, B. D. Schutter, K. Delaney, and J. Connell, Kalman filter-based distributed predictive control of large-scale multi-rate systems: Application to power networks, *IEEE Transactions on Control Systems Technology*, vol. 21, no. 1, pp. 27–39, 2013.

[38] Y. S. Shmaliy, F. Lehmann, S. Zhao, and C. K. Ahn, Comparing robustness of the Kalman, H_∞, and UFIR filters, *IEEE Transactions on Signal Processing*, vol. 66, no. 13, pp. 3447–3458, 2018.

[39] S. Sun, Distributed optimal linear fusion predictors and filters for systems with random parameter matrices and correlated noises, *IEEE Transactions on Signal Processing*, vol. 68, pp. 1064–1074, 2020.

[40] S. Sun, F. Peng, and H. Lin, Distributed asynchronous fusion estimator for stochastic uncertain systems with multiple sensors of different fading measurement rates, *IEEE Transactions on Signal Processing*, vol. 66, no. 3, pp. 641–653, 2018.

[41] D. Svensson, M. Ulmke, and L. Hammarstrand, Multitarget sensor resolution model and joint probabilistic data association, *IEEE Transactions on Aerospace and Electronic Systems*, vol. 48, no. 4, pp. 3418–3434, 2002.

[42] H. Tao, H. Tan, Q. Chen, H. Liu and J. Hu, H_∞ state estimation for memristive neural networks with randomly occurring DoS attacks, *Systems Science & Control Engineering*, vol. 10, no. 1, pp. 154-165, 2022.

[43] Y. Theodor, and U. Shaked, Robust discrete-time minimum-variance filtering, *IEEE Transactions on Signal Processing*, vol. 44, no. 2, pp. 181–89, 1996.

[44] V. Ugrinovskii, and E. Fridman, A Round-Robin type protocol for distributed estimation with H_∞ consensus, *Systems & Control Letters*, vol. 69, pp. 103–110, 2014.

[45] F. Wang, Z. Wang, J. Liang, and X. Liu, Recursive state estimation for two-dimensional shift-varying systems with random parameter perturbation and dynamical bias, *Automatica*, vol. 112, art. no. 108658, 2020.

[46] H. Wang, H. Li, J. Fang, and H. Wang, Robust Gaussian Kalman filter with outlier detection, *IEEE Signal Processing Letters*, vol. 25, no. 8, pp. 1236–1240, 2018.

[47] L. Wang, S. Liu, Y. Zhang, D. Ding, and X. Yi, Non-fragile l_2-l_∞ state estimation for time-delayed artificial neural networks: an adaptive event-triggered approach, *International Journal of Systems Science*, vol. 53, no. 10, pp. 2247-2259, 2022.

[48] G. Wei, W. Li, D. Ding, and Y. Liu, Stability analysis of covariance intersection-based Kalman consensus filtering for time-varying systems, *IEEE Transactions on Systems, Man, and Cybernetics: Systems*, vol. 50, no. 11, pp. 4611–4622, 2020.

[49] W. Xu, D. W. C. Ho, J. Zhong, and B. Chen, Event/self-triggered control for leader-following consensus over unreliable network with DoS attacks, *IEEE Transactions on Neural Networks and Learning Systems*, vol. 30, no. 10, pp. 3137–3149, 2019.

[50] H. Yu, J. Hu, B. Song, H. Liu and X. Yi, Resilient energy-to-peak filtering for linear parameter-varying systems under random access protocol, *International Journal of Systems Science*, vol. 53, no. 11, pp. 2421-2436, 2022.

[51] L. Yu, Y. Cui, Y. Liu, N. D. Alotaibi, and F. E. Alsaadi, Sampled-based consensus of multi-agent systems with bounded distributed time-delays and dynamic quantisation effects, *International Journal of Systems Science*, vol. 53, no. 11, pp. 2390-2406, 2022.

[52] J. Zhang, X. He, and D. Zhou, Filtering for stochastic uncertain systems with non-logarithmic sensor resolution, *Automatica*, vol. 89, pp. 194–200, 2018.

[53] X.-M. Zhang, Q.-L. Han, X. Ge, and L. Ding, Resilient control design based on a sampled-data model for a class of networked control systems under denial-of-service attacks, *IEEE Transactions on Cybernetics*, vol. 50, no. 8, pp. 3616–3626, 2020.

[54] Y. Zhao, X. He, L. Ma, and H. Liu, Unbiasedness-constrained least squares state estimation for time-varying systems with missing measurements under round-robin protocol, *International Journal of Systems Science*, vol. 53, no. 9, pp. 1925-1941, 2022.

[55] W. Zhu, J. Tang, S. Wan, and J. Zhu, Outlier-resistant adaptive filtering based on sparse Bayesian learning, *Electronics Letters*, vol. 50, no. 9, pp. 663–665, 2014.

[56] L. Zou, Z. Wang, Q.-L. Han, and D. Zhou, Recursive filtering for time-varying systems with random access protocol, *IEEE Transactions on Automatic Control*, vol. 64, no. 2, pp. 720–727, 2019.

Hang Geng (Member, IEEE) received the B.Sc. degree in electronic information engineering in 2011 from Civil Aviation Flight University of China, Guanghan, China, the M.Sc. degree in electrical engineering and the Ph.D. degree in control science and engineering in 2014 and 2017, respectively, from Northwestern Polytechnical University, Xi'an, China.

He is currently an Associate Professor in the School of Automation Engineering, University of Electronic Science and Technology of China, Chengdu, China. He was a visiting Ph.D. student (2015-2016) and a Research Fellow (2019-2022) with the Department of Computer Science, Brunel University London, Uxbridge, U.K. From 2018 to 2019, he was a Post-Doctoral Fellow with the Department of Mechanical Engineering, University of Kansas, Lawrence, U.S. His research interests include signal detection and estimation, information processing and fusion, system modeling and estimation, etc.

Dr. Geng is currently serving as Associate Editors for International Journal of Network Dynamics and Intelligence, and CMES-Computer Modeling in Engineering & Sciences; a Senior Member of China Instrument and Control Society; a Member of Chinese Association of Automation; and a very active reviewer for many international journals.

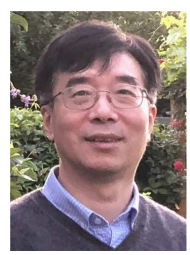

Zidong Wang (Fellow, IEEE) received the B.Sc. degree in mathematics in 1986 from Suzhou University, Suzhou, China, and the M.Sc. degree in applied mathematics in 1990 and the Ph.D. degree in electrical engineering in 1994, both from Nanjing University of Science and Technology, Nanjing, China.

He is currently Professor of Dynamical Systems and Computing in the Department of Computer Science, Brunel University London, U.K. From 1990 to 2002, he held teaching and research appointments in universities in China, Germany and the UK. Prof. Wang's research interests include dynamical systems, signal processing, bioinformatics, control theory and applications. He has published more than 700 papers in international journals. He is a holder of the Alexander von Humboldt Research Fellowship of Germany, the JSPS Research Fellowship of Japan, William Mong Visiting Research Fellowship of Hong Kong.

Prof. Wang serves (or has served) as the Editor-in-Chief for *International Journal of Systems Science*, the Editor-in-Chief for *Neurocomputing*, the Editor-in-Chief for *Systems Science & Control Engineering*, and an Associate Editor for 12 international journals including IEEE Transactions on Automatic Control, IEEE Transactions on Control Systems Technology, IEEE Transactions on Neural Networks, IEEE Transactions on Signal Processing, and IEEE Transactions on Systems, Man, and Cybernetics-Part C. He is a Member of the Academia Europaea, a Member of the European Academy of Sciences and Arts, an Academician of the International Academy for Systems and Cybernetic Sciences, a Fellow of the IEEE, a Fellow of the Royal Statistical Society and a member of program committee for many international conferences.

Jun Hu (Member, IEEE) received the B.Sc. degree in information and computation science and M.Sc. degree in applied mathematics from Harbin University of Science and Technology, Harbin, China, in 2006 and 2009, respectively, and the Ph.D. degree in control science and engineering from Harbin Institute of Technology, Harbin, China, in 2013.

From September 2010 to September 2012, he was a Visiting Ph.D. Student in the Department of Information Systems and Computing, Brunel University, U.K. From May 2014 to April 2016, he was an Alexander von Humboldt research fellow at the University of Kaiserslautern, Kaiserslautern, Germany. From January 2018 to January 2021, he was a research fellow at the University of South Wales, Pontypridd, U.K. He is currently Professor in the Department of Mathematics, Harbin University of Science and Technology, Harbin 150080, China. His research interests include nonlinear control, filtering and fault estimation, time-varying systems and complex networks. He has published more than 80 papers in refereed international journals.

Dr. Hu serves as a reviewer for Mathematical Reviews, as an editor for Neurocomputing, Journal of Intelligent and Fuzzy Systems, Neural Processing Letters, Systems Science and Control Engineering, and as a guest editor for International Journal of General Systems and Information Fusion.

Qing-Long Han (Fellow, IEEE) received the B.Sc. degree in Mathematics from Shandong Normal University, Jinan, China, in 1983, and the M.Sc. and Ph.D. degrees in Control Engineering from East China University of Science and Technology, Shanghai, China, in 1992 and 1997, respectively.

Professor Han is Pro Vice-Chancellor (Research Quality) and a Distinguished Professor at Swinburne University of Technology, Melbourne, Australia. He held various academic and management positions at Griffith University and Central Queensland University, Australia. His research interests include networked control systems, multi-agent systems, time-delay systems, smart grids, unmanned surface vehicles, and neural networks.

Professor Han was awarded The 2021 Norbert Wiener Award (the Highest Award in systems science and engineering, and cybernetics) and The 2021 M. A. Sargent Medal (the Highest Award of the Electrical College Board of Engineers Australia). He was the recipient of The 2022 IEEE SMC Society Andrew P. Sage Best Transactions Paper Award, The 2021 IEEE/CAA Journal of Automatica Sinica Norbert Wiener Review Award, The 2020 IEEE Systems, Man, and Cybernetics Society Andrew P. Sage Best Transactions Paper Award, The 2020 IEEE Transactions on Industrial Informatics Outstanding Paper Award, and The 2019 IEEE Systems, Man, and Cybernetics Society Society Andrew P. Sage Best Transactions Paper Award.

Professor Han is a Member of the Academia Europaea (The Academy of Europe). He is a Fellow of The International Federation of Automatic Control (IFAC) and a Fellow of The Institution of Engineers Australia (IEAust). He is a Highly Cited Researcher in both Engineering and Computer Science (Clarivate Analytics). He has served as an AdCom Member of IEEE Industrial Electronics Society (IES), a Member of IEEE IES Fellows Committee, and Chair of IEEE IES Technical Committee on Networked Control Systems. Currently, he is Editor-in-Chief of IEEE/CAA Journal of Automatica Sinica, Co-Editor-in-Chief of IEEE Transactions on Industrial Informatics, and Co-Editor of Australian Journal of Electrical and Electronic Engineering.

Yuhua Cheng (Senior Member, IEEE) received the Ph.D. degree in instrumentation science and technology in 2007 from Sichuan University, Chengdu, China.

He is currently a Professor of Instrument Science and Technology in the School of Automation Engineering, University of Electronic Science and Technology of China, Chengdu, China. From 2013 to 2014, he was a Guest Researcher at the University of Toronto, Toronto, Canada. His research interests include electronic instrumentation, imaging/sensing for nondestructive evaluation, intelligent prognostics and health management of complex systems, and numerical modeling and simulation.

Prof. Cheng is currently serving as Associate Editors for Neurocomputing and IEEE Transactions on Instrumentation and Measurement; and a very active reviewer for many international journals.